Fusion Engineering and Design 215 (2025) 114936

Contents lists available at ScienceDirect

Fusion Engineering and Design

journal homepage: www.elsevier.com/locate/fusengdes

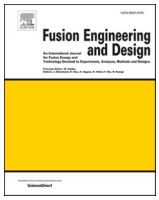

First experimental results of HYDREX operation in hydrogen removal from helium for fusion applications

Vincenzo Narcisi [a,*], Dario Diamanti [b], Daniele Martelli [b], Alessia Santucci [a]

[a] ENEA, Nuclear Department, Frascati Research Centre, 00044 Frascati, Roma, Italy
[b] ENEA, Nuclear Department, Brasimone Research Centre, 40032 Camugnano, Bologna, Italy

ARTICLE INFO

Keywords:
HYDREX facility
Coolant purification system
EU-DEMO
Tritium removal
Copper oxide
Zeolite molecular sieve

ABSTRACT

The tritium removal from gaseous effluents represents a key issue for the deployment of future fusion power plants even more when tritium is present in the order of parts per million. A promising system derives from the fission experience, where oxidizing beds combined with Zeolite Molecular Sieve (ZMS) beds are adopted to purify helium coolant and cover gas. In this work, an integral helium purification process involving these technologies is studied in the Hydrogen Extraction (HYDREX) experimental facility assuming boundary conditions relevant for the Coolant Purification System of the EU-DEMO Helium Cooled Pebble Bed Breeding Blanket. The experimental campaign demonstrates the efficient purification performance allowing the removal of 96 % of the hydrogen. Then, a proper regeneration procedure is experimentally investigated providing a satisfactory restoring of the adsorption capability of the zeolite material. Some open aspects are individuated, mainly related to the uneven distribution of the flow through the ZMS bed causing an earlier saturation of the bed and a not completed regeneration of the zeolite material. Furthermore, a huge release of hydrogen in the first minutes of the regeneration is experienced due to the not completed oxidation. The results obtained in this work are relevant for the definition of further experimental investigations and as guidelines for the design of gas detritiation systems.

List of acronyms

ADS	Adsorption
CM	Compressor
CPS	Coolant Purification System
FM	Flow Meter
HCPB	Helium Cooled Pebble Bed
HTTR	High Temperature Engineering Test Reactor
HYDREX	Hydrogen Extraction
LFMR	Liquid Metal-cooled Fast Reactor
MFC	Mass Flow Controller
MS	Mass Spectrometer
NA	Not available
PHTS	Primary Heat Transport System
RB	Reducing Bed
REG	Regeneration
TBM	Test Blanket Module
TES	Tritium Extraction System

1. Introduction

Among the reactions considered to be exploited in future fusion machines, deuterium-tritium is recognized as the most promising one due to its highest cross section at lowest energy. Nevertheless, the use of tritium poses some challenges, mainly related to its radioactivity. One of these is the availability of tritium for fusion machines [1], taking into account that, for example, a 2 GW fusion power plant like EU-DEMO is expected to consume around 112 kg of tritium per full power year [2]. Tritium is a pure beta emitter with a half-life of 12.3 years and is currently generated in CANDU-type reactors with a rate of around 130 grams per year for a typical CANDU reactor. However, there is a significant uncertainty about the future tritium production since the actual CANDU fleet is expected to phase out in the coming decades [1].

The engineering answer to the tritium availability concern is the Breeding Blanket [2]. Among other functions, the Breeding Blanket must breed enough tritium to ensure the tritium self-sufficiency. To do this, a relevant quantity of tritium is produced inside this component by capturing fusion neutrons in lithium-bearing materials. Meanwhile, the

* Corresponding author.
E-mail address: vincenzo.narcisi@enea.it (V. Narcisi).

https://doi.org/10.1016/j.fusengdes.2025.114936
Received 20 November 2024; Received in revised form 21 January 2025; Accepted 4 March 2025
Available online 9 March 2025

Breeding Blanket adsorbs most of the fusion energy transported by neutron from plasma that must be recovered by the Primary Heat Transport System (PHTS) for energy production purpose. To do this, the Breeding Blanket is characterized by large and thin metallic heat transfer surfaces surrounded by high temperatures and highly tritiated environment. These represent favourable conditions for tritium permeation from Breeding Blanket into PHTS resulting in the contamination of the primary coolant [3]. Once in the PHTS, tritium can migrate towards rooms and environment via leaks and further permeation. Thus, a proficient Coolant Purification System (CPS) is essential to avoid the tritium build-up inside the PHTS and the issues related to its migration path [3].

During the EU-DEMO pre-concept design phase, two Breeding Blanket concepts were identified [4]. Among these, the Helium Cooled Pebble Bed (HCPB) is characterized by a solid breeder cooled by helium at 8 MPa and 300–520 °C. The present paper focuses on the most promising technologies considered for the purification of the primary helium from tritium permeated from the Breeding Blanket, based on a batch operation of copper oxide (CuO) and Zeolite Molecular Sieve (ZMS) beds. In the following sections the process will be presented and the main outcomes of an integral experimental activity conducted in the Hydrogen Extraction (HYDREX) facility will be discussed.

2. The helium purification process

The process considered for the EU-DEMO primary helium purification is derived from the experience of the helium-cooled fission reactors, where impurities must be removed from the primary coolant to avoid oxidation and corrosion of moderator and structural materials. The case of the High Temperature Engineering Test Reactor (HTTR) [5] and of the High Temperature Reactor HTR-10 [6] are taken as reference. The reactors were equipped with a CPS for the coolant purification from impurities (e.g., hydrogen, carbon monoxide, water vapour and carbon dioxide). For the hydrogen removal (all the isotopes, including tritium), the CPS relying on the combination of copper oxide and zeolite molecular sieve beds. The copper oxide fixed bed, operating at 250–280 °C, burns all the hydrogen isotopes into water and the ZMS bed, operated at ambient temperature, adsorbs the so-formed water vapor. The entire process ensures a purification efficiency of around 99 % [5,6]. Then, in the regeneration phase, the copper oxide bed is subjected to an oxygen throughput at 80 °C whereas the ZMS bed is purged with a helium flow rate at 280 °C so that the adsorbed water is released. The final recovery of tritiated water is fulfilled with a cooler and a moisture separator [6].

Based on this return of experience, a conceptual design of the EU-DEMO helium CPS has been derived [7]. Such a design was based on the following hypotheses: (i) almost all the hydrogen isotopes are oxidized in the CuO bed, (ii) almost all the tritiated water is adsorbed in the ZMS, (iii) around 60 % of the exhaust copper can be reduced in the regeneration process, (iv) all the adsorbed tritiated water can be theoretically released during regeneration of ZMS bed, and (v) an ideal behaviour of the ZMS in both the adsorption and the regeneration phases. The reliability of the CPS design needs experimental verification of these assumptions.

Although these technologies are already adopted in fission and industrial applications, especially the ZMS in pharmaceutical and cryogenic industries [8–11], experimental data related to the integral operation of this purification process are poorly reported in literature. For example, Gorbach et al. presented the experimental acquisition of breakthrough curves of water molar fraction during the adsorption into ZMS, but no information is reported about the regeneration phase [12]. In fact, in most of the cases, ZMS beds are used for humidity removal purpose, therefore regeneration is not a phase that is deeply investigated. However in fusion applications, being the adsorbed water tritiated, the understanding of the regeneration phase is crucial for the definition of the tritiated water inventory and for the detritiation process. In this framework, the HYDREX test facility offers a unique opportunity to test an integral purification process under fusion relevant conditions.

2.1. The HYDREX facility

HYDREX is a multifunctional facility aimed at testing technologies and processes relevant for gas detritiation. The facility (Fig. 1) was commissioned and constructed at the ENEA Brasimone Research Centre, in the ambit of the Framework Partnership Agreement F4E-FPA-380, Action 1, Specific Grant 01, to support the ITER Test Blanket Module (TBM) programme, but it can be used also for the development of Liquid Metal-cooled Fast Reactors (LMFR) [13]. The apparatus is relevant for the CPS and the Tritium Extraction System (TES) of helium-cooled TBMs along with the purification system of the LMFR cover gas.

A simplified process flow diagram of the facility is presented in Fig. 2a. It includes two oxidizing beds (CUO01 and CUO02 in Fig. 2) connected in series (see Fig. 1b). Each one has a length of 3 m and a diameter of 38 mm. For the present experimental campaign, these beds are filled with copper oxide (CuO, 3 kg per each bed) but different oxidizing materials can be tested. The zeolite molecular sieve bed (ZMS in Fig. 2) consists of the MicroTorr purifiers MC700 provided by SAES getters. It is a 316 L stainless steel cylinder with a diameter of 76 mm and a length of 254 mm (see Fig. 1c), designed for nominal and maximum flow rate of 1.5 and 7 $Nm^3\ h^{-1}$, respectively, and a maximum operating pressure of 17.3 barg and allows to test several types of molecular sieves. The bed is equipped with two metal filters having porous of 2.0 μm, these are located inside the purifier at both the edges working also as support for the internals. Depending on the purification task, the MicroTorr purifier can be filled with different materials and thus, several types of molecular sieves can be tested. For the present campaign the purifier is filled with 500 g of zeolite 3A, collected between the two metal filters.

The main characteristics of the oxidizing and of the molecular sieve materials used in the experimental campaign are summarized in Table 1. Although not used in the present campaign and not reported in Fig. 2, the facility is also equipped with a Reducing Bed (RB) that can be filled with metallic getter to test their performance in the reduction of the water released during the ZMS regeneration.

In the present setup, the facility uses helium as operational gas and hydrogen to simulate radioactive tritium, but other technical gases can be used (e.g., N_2 or Ar as operative gas and CO or CO_2 as impurities). Helium is sent from dedicated cylinders whereas hydrogen is provided by a hydrogen generator that can ensure an outlet pressure from 0.1 to 1.1 MPa and a throughput up to 0.06 $Nm^3\ h^{-1}$. The inlet flow rate of technical gases is controlled by Mass Flow Controllers (MFC) and the flow rate through the facility is monitored with two Flow Meters (FM). Operative range and accuracy of these instrumentations are summarized in Table 2. Furthermore, all the beds, along with the pipeline indicated in red in Fig. 2, are equipped with heating cables to ensure the proper operative temperatures (see Fig. 1c), acquired by K-type thermocouples with an accuracy of ± 1.5 °C. Furthermore, several pressure monitoring points are present with pressure transducers characterized by an accuracy of 0.5 % LPC.

HYDREX can work in two operational modes, namely the purification and the regeneration. During the purification phase the facility is operated in closed loop (see Fig. 2b). The helium is recirculated inside the facility via the compressor (CM in Fig. 2) and the desired throughput is controlled by two regulating valves and monitored with the FM02. The FM01 measures the total flow rate elaborated by the compressor that is partially recirculated through the bypass line to ensure the correct throughput towards the beds. Upstream the CUO01, the proper hydrogen throughput is mixed with the helium flow rate, obtaining the desired composition. The gas mixture is pre-heated and enters the two CuO beds where the hydrogen molecules are oxidized into water. Then, the mixture consisting in helium and water humidity flows through 24 m long piping exposed to ambient temperature to cool down the gas before the ZMS that, operating at ambient temperature, adsorbs the water

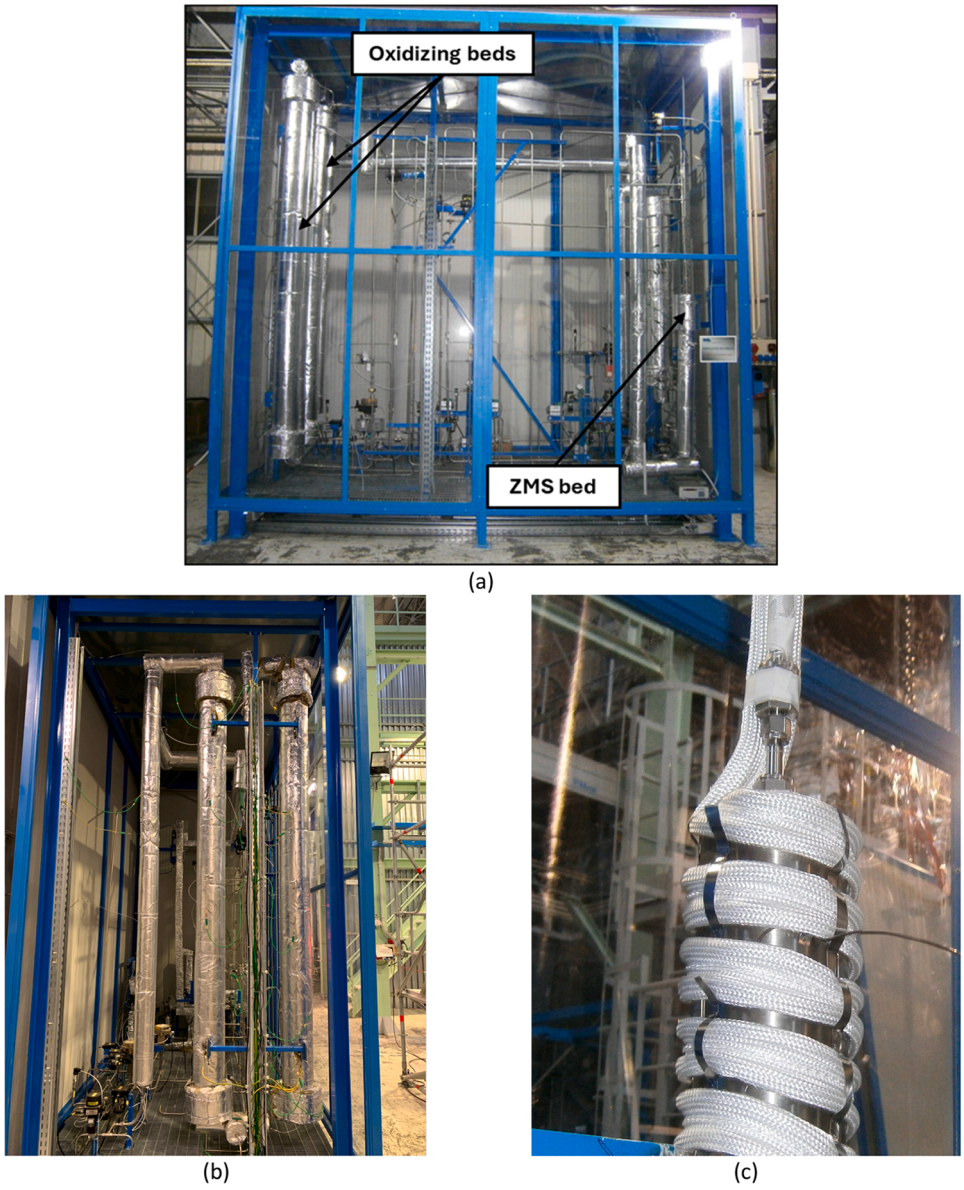

Fig. 1. The HYDREX test facility: view of the integral process (a), details of the oxidizing beds (b) and of the zeolite molecular sieve bed (c).

content returning pure helium at the outlet. The loop is closed by the compressor and the process is repeated until the ZMS is saturated, namely when the water content in the gas phase is in equilibrium with the water loaded in the ZMS solid phase. To analyse the gas composition, there are two bleeding points which sent a small fraction of the flow rate to the Mass Spectrometer (MS). Referring to Fig. 2b, the bleeding point upstream the ZMS allows to assess the oxidation efficiency of the CuO beds whereas, the second bleeding, downstream the ZMS, provides the evaluation of the purification efficiency. By means of a dedicated pressure control system, the amount of gas sent to the MS is replaced with pure helium from cylinders.

HYDREX is designed to test an integral purification and regeneration procedure but, in the current campaign, only the ZMS has been considered during the regeneration. Thus, in regeneration mode HYDREX is operated in open loop and the purge helium flow rate, typically few percentages of the purification throughput, is sent from the cylinders to the ZMS. The bed is purged in counter current with respect to the purification phase and, the resulting mixture is analysed with the MS and then, released in the environment. The regeneration continues until the whole water content in the ZMS solid phase is released. For further information about the rationale of this process, please refer to the work of Narcisi and Santucci [7].

The main operative parameters of the present experimental campaign are reported in Table 3. The sensitivity analysis has regarded the helium flow rate in both the purification and the regeneration processes whereas the inlet hydrogen partial pressure has been selected to be relevant for the EU-DEMO helium CPS [7].

3. The experimental campaign

The proposed experimental campaign aims at investigating the integral purification process and the regeneration of the ZMS bed under relevant conditions of the EU-DEMO helium CPS. To do this, HYDREX is preliminary prepared with the calibration of the MS and the cleaning of the facility. The MS is calibrated using certified gas mixtures with compositions in terms of helium, hydrogen and water close as much as possible to the ones expected during the different phases of the experiment. Furthermore, the cleaning procedure must ensure the elimination of all the impurities contained in the system, mainly water. The procedure consists of several vacuum and heating operations followed by

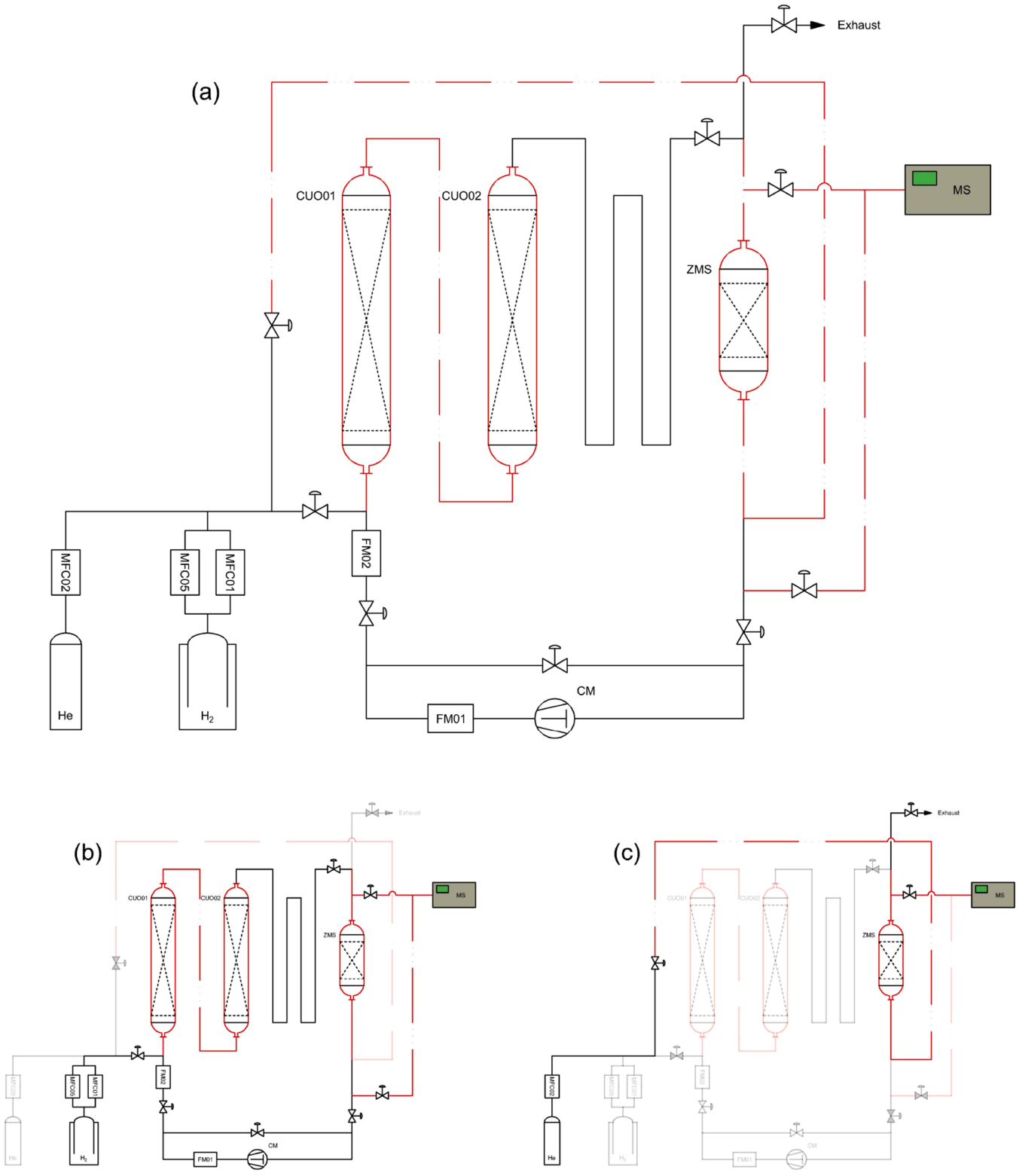

Fig. 2. HYDREX test facility: (a) process flow diagram, (b) adsorption mode, (c) regeneration mode.

fillings with helium, until the residual impurity content is below the desired value. Typically, the background concentration of hydrogen and water are 10^{-6} ppm and 10^{-4} ppm, respectively.

The campaign consists in four adsorption (ADS) and three regeneration (REG) tests, repeated twice (except for the ADS-04), in which the operative conditions are kept as summarized in Table 3 and the helium flow rate is changed as reported in Table 4. Note that the helium purge throughput during regeneration is 10, 5, and 2 % of the maximum purification flow rate of 7 $Nm^3\ h^{-1}$.

The main results of the ADS tests are reported in Figs. 3 and 4 in terms of breakthrough curves of molar fraction of water and in terms of gas temperature value at the ZMS outlet. For sake of clarity, only one of the two series of tests is reported in the figures, being the second one comparable. During the breakthrough, the water content in the ZMS

Table 1
Main characteristics of oxidizing and molecular sieve material used in the present experimental campaign.

Material	Product	Supplier	Description
CuO	PuriStar® R3–11 G T5×3	BASF	Tablet: nominal diameter of 5 mm and height of 3 mm, approximately 45 % of CuO Bulk density: 900 kg m^{-3}
ZMS 3A	SYLOBEAD® MS 564 C	Grace Davison	Pellet diameter: 1.6–3.15 mm Bulk density: 720 kg m^{-3}

Table 2
List of mass flow controllers and flow meters.

Component	Operative range	Accuracy
MFC01	7.5 10^{-5}–3.75 10^{-3} Nm^3h^{-1}	± 0.5 % of reading plus ± 0.1 % of full scale
MFC02	0.05–2.5 Nm^3h^{-1}	
MFC05	1 10^{-3}–0.05 Nm^3h^{-1}	
FM01	0.4–20 Nm^3h^{-1}	
FM02	0.24–12 Nm^3h^{-1}	

Table 3
Main operative parameters.

Parameter	Unit	Purification	Regeneration
Total pressure	MPa	0.8	0.22
H_2 inlet partial pressure	Pa	640	–
He flow rate	Nm^3h^{-1}	1.5–7	0.14–0.7
CuO temperature	°C	250	–
ZMS temperature	°C	20	300

Table 4
The experimental test matrix.

Test ID	He flow rate (Nm^3h^{-1})
ADS-01	7.00
ADS-02	5.00
ADS-03	3.00
ADS-04	1.50
REG-01	0.70
REG-02	0.35
REG-03	0.14

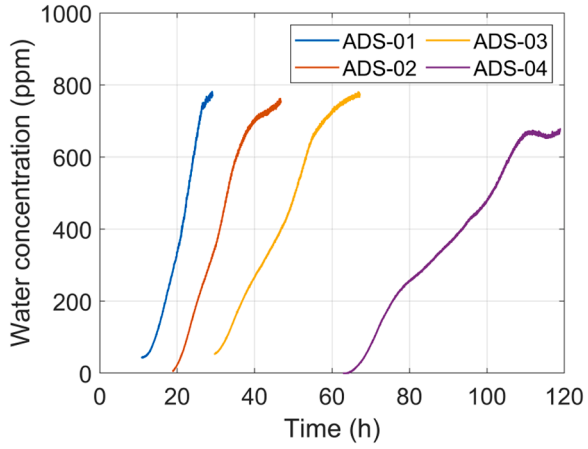

Fig. 3. Breakthrough curves of molar fraction of water at ZMS outlet during adsorption tests.

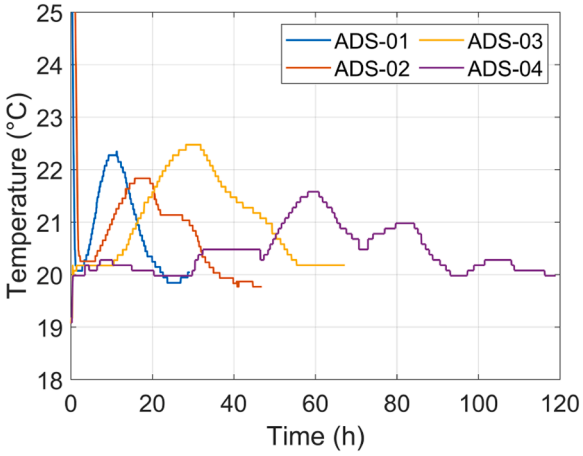

Fig. 4. Gas temperature at ZMS outlet during adsorption test.

outlet stream increases. Thus, a control system is implemented in the facility to modulate the hydrogen feed flow rate coming from the generator and to ensure a constant molar fraction of water at the ZMS inlet over the whole test.

Looking at the breakthrough curves of the molar fraction of water (Fig. 3), the first outcome is that the complete saturation of the ZMS is delayed by decreasing the flow rate and as expected, the saturation time is inversely proportional to the throughput. The purification efficiency of the integrated process can be evaluated from the composition at the ZMS outlet before the breakthrough. The molar fraction of hydrogen (not reported in Fig. 3) is null over the whole test thus, the purification efficiency (η_p) can be defined as:

$$\eta_p = \frac{c_{H2,\ in} - c_{H2O,\ out}}{c_{H2,\ in}} \cdot 100 \quad (1)$$

where $c_{H2,in}$ is the molar fraction of hydrogen before oxidation, calculated as the ratio between the hydrogen flow rate elaborated by MFC01 or MFC05 (depending on the test) and the throughput measured by FM02 (see to Fig. 2), and $c_{H2O,out}$ is the molar fraction of water measured by the MS at the ZMS outlet before the breakthrough. Referring to Fig. 3, before the breakthrough a residual water content is visible for tests ADS-01 and ADS-03 whereas a null molar fraction of water is obtained for ADS-02 and ADS-04, resulting in a purification efficiency of 96 and 100 %, respectively. It is worth mentioning that, for a well calibrated instrument and for high values of concentration, the accuracy of the MS can be considered equal to 0.25 %. Nevertheless, this value increases for concentrations in the order of magnitude of ppm and the accuracy of the calibration depends on the ambient conditions. In this case, the calibration is carried out at the beginning of a series of tests and thus, it could affect the accuracy of the measurement, and this could partially explain the discrepancy in terms of purification efficiency. Although this spread, it is reasonable to say that a purification efficiency higher than 95 % can be expected from this process.

From a qualitative point of view, a non-ideal adsorption is shown in Figs. 3 and 4. The breakthrough of the molar fraction of water presents a couple of humps in each test which are more visible in the cases at lower flow rate. The behaviour can be explained by a non-uniform distribution of the flow in the radial direction of the bed that becomes more relevant when the throughput and thus, the superficial velocity through the bed, decreases. This leads to multiple fronts of reactions which are visible in the breakthrough of the gas temperature at the ZMS outlet. In fact, the water adsorption in the ZMS is an exothermic reaction and when the mass transfer zone reaches the outlet region of the bed (the breakthrough occurrence) an increase in the outlet temperature is visible. Theoretically, the breakthrough of the gas temperature should be characterized by a single peak but in this case multiple peaks are visible

(see Fig. 4).

For sake of comparison, the experimental trends of the breakthrough curves of ADS-02 are compared with simulation results (black dashed line) in Figs. 5 and 6 for the molar fraction of water and for the gas temperature, respectively. The simulations are performed with a dynamic model presented in reference [7]. The simulation matches well with the experimental trend in the second part of the breakthrough demonstrating that the time required for the complete saturation of the ZMS is not affected by the non-ideal adsorption. Nevertheless, such non-ideal behaviour affects the time at which the breakthrough starts. Compared with the simulation (see Fig. 5), the experimental breakthrough begins about eight hours earlier due to the first front of reaction (Fig. 6). This kind of information is of great interest for the design of the EU-DEMO helium CPS since the switch of the bed from adsorption to regeneration must be activate as soon as the breakthrough arises to avoid the release of tritiated water.

From a quantitative point of view, the main results are reported in Table 5 where (i) and (ii) individuates the two series of tests. For sake of comparison, the theoretical equilibrium water loading in ZMS under the operative conditions reported in Table 3 is equal to 126 NL. As better described in the follow, the discrepancy between the expected water load and the measured one can be explained by several reasons related to the features of the experimental setup, the material degradation and the regeneration efficiency.

As said above, two bleeding points are alternatively available, before and after the ZMS. The amount of water adsorbed in the ZMS is obtained by the difference between the amount of water entering and exiting the ZMS. Being impossible to measure at the same time the inlet and outlet water concentration two assumptions are considered. When monitoring the ZMS inlet, the purification efficiency is assumed 100 % (no water at the ZMS exit) instead, when monitoring the ZMS outlet, the amount of water entering the ZMS is obtained by linear extrapolation. Regarding the ZMS packing material, it has to be considered the aging effect that reduces the adsorption capability [14]. Finally it is worth emphasizing that, especially in the first hours of the test, the ZMS inlet water content is not constant being affected by the water accumulation inside the CuO beds. These, along with the uncertainty in the regeneration efficiency performed before the adsorption, lead to an uncertainty that is difficult to quantify.

The oxidation efficiency (η_{CUO}) is evaluated as:

$$\eta_{CUO} = \frac{C_{H2,\,p} - C_{H2,reg}}{C_{H2,\,p}} \cdot 100 \quad (2)$$

where $C_{H2,p}$ is the integral amount of hydrogen sent to the facility during the purification test and $C_{H2,reg}$ is the integral amount of hydrogen released during the following ZMS regeneration. This latter parameter will be clarified analysing the outcomes of the regeneration tests. Table 5 demonstrates the high performances of the CuO to oxidize hydrogen into water with a high repeatability of around 98.7 %.

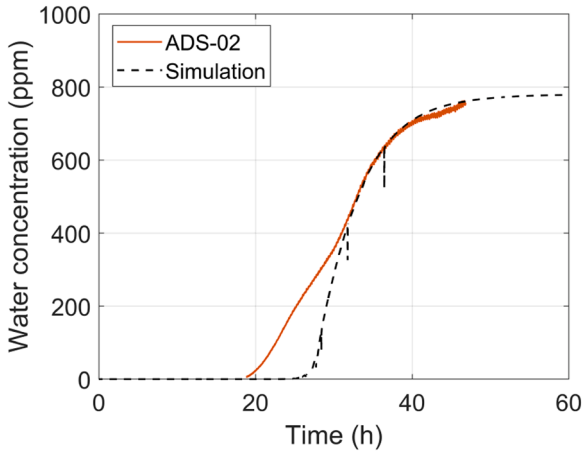

Fig. 5. Breakthrough curves of molar fraction of water at ZMS outlet: comparison between ADS-02 and simulations.

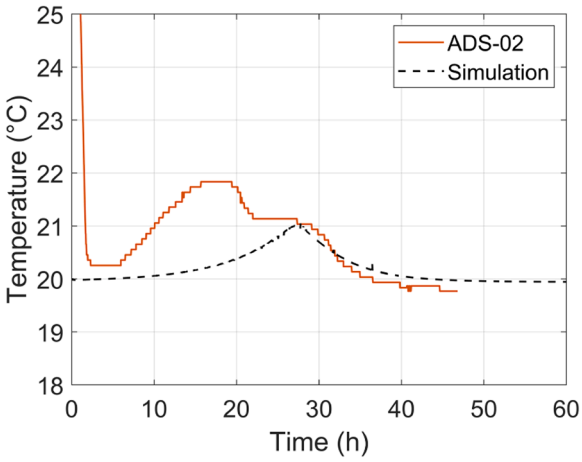

Fig. 6. Gas temperature at ZMS outlet: comparison between ADS-02 and simulations.

Table 5
Main quantitative results of the ADS tests: amount of water adsorbed into the ZMS and oxidation efficiency of the CuO.

Test ID	Adsorbed water (NL)	Oxidation efficiency (%)
ADS-01 (i)	96.86	NA
ADS-01 (ii)	83.00	91.94
ADS-02 (i)	88.70	98.64
ADS-02 (ii)	77.57	97.78
ADS-03 (i)	98.34	98.81
ADS-03 (ii)	80.00	98.63
ADS-04 (i)	105.00	98.66

Once the ZMS is saturated, the regeneration phase starts with the depressurization of the ZMS followed by a 10 °C h^{-1} warm-up. A purge helium flow rate is continuously sent to the bed as specified in Table 4. Generally, the superficial velocity and thus, the linear pressure drop, are key design parameters for a packed bed and must range between a minimum value to prevent channelling and a maximum value to avoid too high pressure drop and the consequent damage of the sieving material [14]. It is worth mentioning that in common applications, such as pharmaceutical and cryogenic industries, the objective is the production of ultra-pure components via water removal. In these processes, the regeneration phase aims at the restoration of the adsorption capabilities of the molecular sieve bed that shall be fulfilled in the most efficient way. The helium CPS and more in general, detritiation systems of gaseous effluents, add to the purification purpose the need of the final recovery of the tritiated water produced during the molecular sieve regeneration and collected via moisture separator. To facilitate the condensation, high concentrations of water are preferable and thus, the purge gas flow rate should be minimized. The minimum linear pressure drop is assumed 230 Pa m^{-1} [14] and the Ergun equation, which relates linear pressure drop to superficial velocity [15], is adopted for the definition of the flow rate for the experiment. Referring to the throughputs reported in Table 4, the associated linear pressure drops are 610, 303, and 121 Pa m^{-1} for REG-01, REG-02, and REG-03, respectively. The intent of REG-03 is to investigate the effect of too low purge flow rate.

Fig. 7 shows the molar fraction of water over the whole regeneration phase for the three cases. Instabilities in the regeneration process are visible for the REG-03 case, presumably due to an uneven distribution of the purge flow rate through the zeolite material. Such discontinuities are

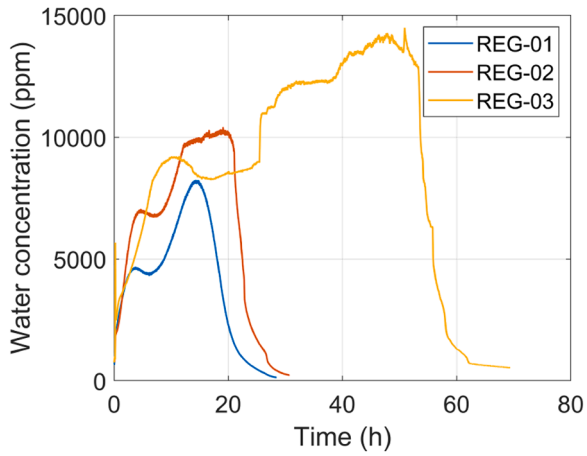

Fig. 7. Molar fraction of water at the ZMS outlet during regeneration tests.

less relevant in the REG-02 and disappear in REG-01. After the first three hours, when the water release rate is similar in the three tests, the water concentration stabilizes to three different values, increasing from 4590 to 9124 ppm from REG-01 to REG-03, and then increases again up to the maximum value reached just before the end of the process. Such value divided by the hydrogen feed concentration during the purification phase, provides the enrichment ratio, an important figure of merit of the integral purification and regeneration process. This parameter provides the effectiveness of the entire process, higher is the enrichment ratio easier will be the water recovery in the moisture separator. For REG-01, REG-02, and REG-03 this parameter assumes the value of 10, 13, and 18, respectively.

Another figure of merit is the time needed for the regeneration of the bed, which impacts on the number of beds required to ensure a continuous operation of the detritiation system (see reference [7] for more details). The choice of the purge gas flow rate shall derive from a compromise between the enrichment ratio and the time needed for the regeneration. Considering the heating rate applied to the walls of the bed, the ZMS reaches the nominal regeneration temperature after 28 h from the beginning of the process. Based on the outcomes of the pre-test simulations, this time is expected to be enough for the complete regeneration in all the analysed cases. As presented in Fig. 8, where the experimental data of REG-01 and REG-02 are compared with simulation results, this is true for these two cases, whose time needed for regeneration differs of around 2 h. On the other hand, for the REG-03 the uneven distribution of the purge flow rate causes a huge delay in the end of the process which lasts >60 h (see Fig. 7).

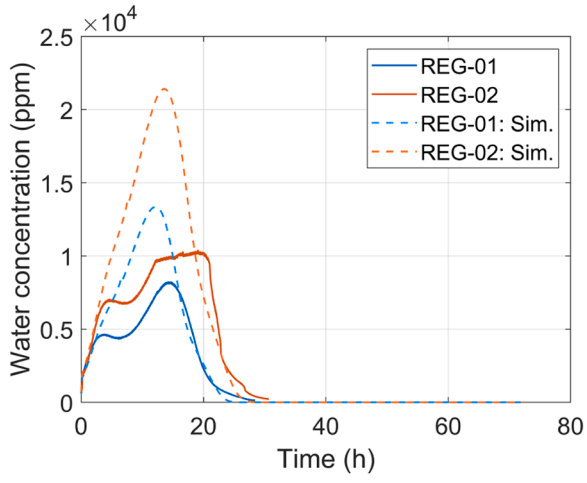

Fig. 8. Molar fraction of water at the ZMS outlet: comparison between REG-01, REG-02, and simulations.

Focusing on the comparison between the experimental data and the simulation results, although the first and the latest hours are well reproduced, a huge discrepancy is observed in the central part of the process (see Fig. 8) which results in a water release lower than expected. The integral amount of water released during the regeneration tests and the efficiency of this process are summarized in Table 6. The regeneration efficiency is evaluated as the ratio between the water released during regeneration (Table 6) and the water adsorbed during purification (Table 5) and ranges between 80 and 95 %. It is worth noting that the efficiency decreases even more if referred to the theorical equilibrium loading of 126 NL instead of the water adsorbed in the purification process and such a discrepancy is represented by the difference between the areas subtended to the experimental and the simulation trends in Fig. 8.

The explanation of this discrepancy can be obtained from the experimental acquisition of gas temperature at the inlet and outlet of the ZMS, reported in Fig. 9. It is worth considering that the regeneration process is an endothermic reaction characterized by a heat of reaction in the range of 58 and 60 kJ mol^{-1} [16] which is provided by the heating cables installed on the outside walls and by the hot purge gas entering the bed. Theoretically, the regeneration process is concluded when the temperature of the outlet gas mixture equals the inlet value of 300 °C, meaning that release reactions are completed. Looking at Fig. 9, a huge discrepancy between the inlet and the outlet temperature is observed, ranging from 97 °C in the best case (REG-01) to154 °C in the worst case (REG-03). The results shown in Fig. 9 suggest a non-uniform temperature distribution inside the bed. The zeolite material is heated from the outside walls and thus, a radial profile is expected. Furthermore, hot purge gas is injected from the bottom producing an axial temperature profile depending on the flow rate and on the heat of reaction. These effects lead to a complex temperature profile inside the bed causing the lower outlet temperature highlighted in Fig. 9. As a matter of fact, at the end of the regeneration, only part of the zeolite material reaches the desired temperature explaining the incomplete regeneration. This phenomenon is not fully described in the actual simulation based on a one-dimensional approach which, although considering the axial profile derived by the hot gas flow rate and the heat of reaction, does not account for the radial temperature profile.

A final remark regards the interaction between the hydrogen and the zeolite 3A, already studied and reported in literature in the frame of hydrogen storage and transportation [17–20], and of natural gas purification [21]. The synthetic zeolite is a microporous aluminosilicate where the AlO_2 group introduce a negative charge which is compensated by an additional cation forming a crystal unit. A combination of these units generates the three-dimensional crystalline structure characterized by a central cage (i.e., the α cage) and additional smaller cages (i.e., β cages). The possibility for a molecule to enter the cages of the zeolite is regulated by the type of cation added to the crystalline framework that determines the dimensions of the openings and thus, give the selectivity. Zeolite 3A is a synthetic crystalline obtained adding potassium ion (K^+). It presents one α cage with a free diameter of 11.4 Å, accessible through six 3 Å openings, and eight β cages with a free diameter of 6.6 Å entered through hexagonal windows with a mean effective opening of 2.2 Å [22]. Water presents a mean diameter of 2.7 Å and can easily enter α

Table 6
Main quantitative results of the REG tests: amount of water released during regeneration of ZMS and regeneration efficiency.

Test ID	Released water (NL)	Regeneration efficiency (%)
REG-01 (i)	79.40	75.62
REG-01 (ii)	66.74	83.42
REG-02 (i)	78.70	80.03
REG-02 (ii)	65.71	84.71
REG-03 (i)	82.80	93.35
REG-03 (ii)	65.82	79.30

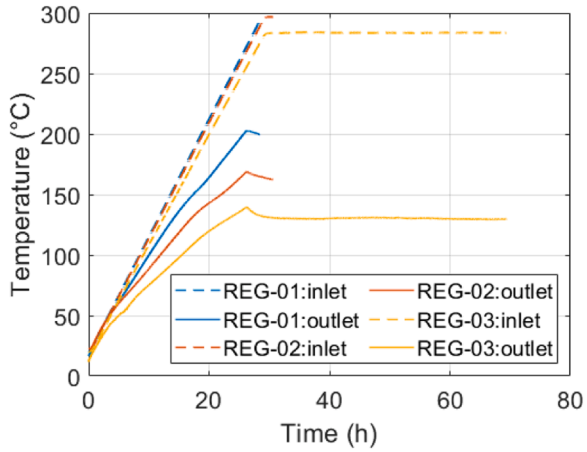

Fig. 9. Gas temperature at the inlet and outlet section of the ZMS during regeneration tests.

cage but also β cages, by displacement of K^+ ion. In the fully hydrated form, the zeolite 3A crystalline can contain 192 molecules of water. Although polar molecules (like water) are preferably attracted (even if the crystalline structure is globally neutral, a high electrical field occurs close to the cations), also non-polar molecules can be adsorbed as long as their dimensions are compatible with the cage openings. This is the case of the hydrogen which presents a dynamic diameter of 2.9 Å. Yang et al. [21] studied the hydrogen uptake in zeolite 3A deriving the adsorption isotherms at different temperature ranging between 20 and 65 °C for pressure between 0 and 1000 kPa. They found that the accessibility of adsorption sites of zeolite 3A to hydrogen is nonmonotonically temperature dependent. Accordingly with the conventional thermodynamics, it decreases by increasing the temperature but below 25 °C the trend is almost specular denoting the presence of a critical admission temperature below this value. Based on this, the zeolite 3A is expected to adsorb the hydrogen present in the feed gas mixture with an equilibrium loading that is lower than the value for water.

Fig. 10 shows the molar fraction of hydrogen in the gas exiting the ZMS during the first 30 min of the three regeneration tests. The ZMS is still at 20 °C and the desired purge gas flow rate is sent through the bed. As the purge gas enters the ZMS, almost all the hydrogen adsorbed during the purification phase is released in few minutes, causing a high molar fraction at the bed exit. Integrating these peaks, it is possible to evaluate the amount of hydrogen adsorbed (Table 7) thus derive the oxidation efficiency expressed by Eq. (2).

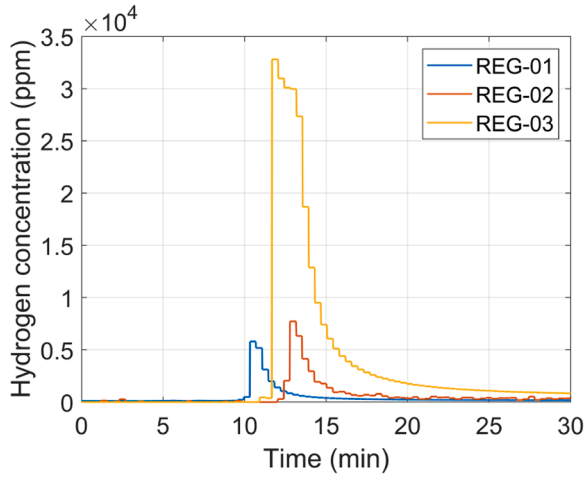

Fig. 10. Molar fraction of hydrogen at the ZMS outlet during the first 30 min of the regeneration tests.

Table 7
Amount of hydrogen released during regeneration of ZMS.

Test ID	Released hydrogen (NL)
REG-01 (i)	1.50
REG-01 (ii)	1.25
REG-02 (i)	1.28
REG-02 (ii)	2.02
REG-03 (i)	1.65
REG-03 (ii)	4.49

The results presented in Fig. 10 gives interesting information: (i) the oxidation efficiency is not 100 % but (ii) the purification efficiency of the whole system is not affected since the ZMS is able to adsorb the residual hydrogen content, and (iii) in the ZMS regeneration a huge release of gaseous tritiated hydrogen shall be expected in the first minutes of the process and a method to manage it shall be foreseen.

4. Conclusions

The paper has shown an experimental assessment of an integral process for detritiation of gaseous effluents proposed for the Coolant Purification System of the EU-DEMO HCPB Breeding Blanket. The activity has been carried out in HYDREX facility, hosted at the ENEA Brasimone Research Centre. The main components are the oxidizing beds, filled with CuO tablets, and the ZMS bed, containing pellets of zeolite 3A. The facility aims at studying the integral helium purification process and the regeneration of the ZMS bed.

The experimental campaign has demonstrated the capabilities of this process to purify the helium stream from low concentrations of hydrogen and to recover the water produced in the process. During the purification, the CuO beds allow the oxidation of around 99 % of the hydrogen throughput and the water formed, along with the residual hydrogen content, are adsorbed in the ZMS bed. The high purification efficiency of the integral process has been confirmed, being higher than 96 %. The purification has been analysed changing the feed flow rate in the operative range of the ZMS bed. As expected, the time before the ZMS saturation is inversely proportional to the throughput but, reducing the flow rate the uprising of multiple fronts of reactions cause the beginning of the breakthrough earlier than expected. Such results confirm the applicability of these technologies for the helium detritiation purpose but highlight the need for an optimisation of the flow conditions through the bed.

The regeneration of the ZMS has been studied for different purge gas flow rates ranging between 2 and 10 % of the maximum allowable throughput. The objective is to reduce as much as possible the purge flow rate and thus, to maximize the final water concentration. The process has demonstrated a high regeneration efficiency, ranging from 75 to 94 %. Nevertheless, some discontinuities have been observed, more relevant for the lowest throughput, leading to an uneven distribution of the flow inside the bed and a not uniform temperature in the zeolite material that cause a not complete regeneration. Furthermore, a large release of hydrogen has been experienced in the first minute of the regeneration. Such outcomes should be further investigated and shall be considered in the design of a proper detritiation system. The dimensions of the bed, along with the purge flow rate, should be optimized to allow a uniform temperature distribution and a proper regeneration, and a strategy to manage the hydrogen release should be identified. For such reasons modelling activities are ongoing to better describe the non-ideal phenomena observed in this experimental campaign.

The present activity has proven the capability of this process to recover most of the hydrogen from an extreme diluted gaseous effluent. In this paper the application for the coolant purification has been considered but, referring to a future fusion machine, the capabilities of this technology can be exploited whenever there is the need for a final detritiation of gaseous streams. Typical applications could be the final

separation stage of the plasma chamber exhaust, regardless of the type of the machine (e.g., tokamak and stellarator), or for the air and vent detritiation of rooms and glove boxes. For these cases, a system like HYDREX could recover the residual tritium content from the exhausted stream providing the dual positive effect of recovering tritium to be used as fuel and of reducing the radiological load to the stack.

CRediT authorship contribution statement

Vincenzo Narcisi: Writing – original draft, Validation, Software, Methodology, Investigation, Formal analysis, Data curation, Conceptualization. **Dario Diamanti:** Writing – review & editing, Supervision, Software, Methodology, Investigation, Formal analysis, Conceptualization. **Daniele Martelli:** Writing – review & editing, Supervision, Methodology, Investigation. **Alessia Santucci:** Writing – review & editing, Supervision, Resources, Project administration, Methodology, Investigation, Funding acquisition, Conceptualization.

Declaration of competing interest

The authors declare the following financial interests/personal relationships which may be considered as potential competing interests:

Vincenzo Narcisi reports financial support was provided by EUROfusion. If there are other authors, they declare that they have no known competing financial interests or personal relationships that could have appeared to influence the work reported in this paper.

Acknowledgements

The authors wish to thank Massimo Valdiserri, Luca Rapezzi, Daniel Gianotti, and Lorenzo Laffi for their precious work in supporting the execution of the experimental campaign.

This work has been carried out within the framework of the EUROfusion Consortium, funded by the European Union via the Euratom Research and Training Programme (Grant Agreement No 101052200—EUROfusion). Views and opinions expressed are However, those of the author(s) only and do not necessarily reflect those of the European Union or the European Commission. Neither the European Union nor the European Commission can be held responsible for them.

Data availability

Data will be made available on request.

References

[1] R.J. Pearson, A.B. Antoniazzi, W.J. Nuttall, Tritium supply and use: a key issue for the development of nuclear fusion energy, Fusion Eng. Des. 136 (2018) 1140–1148, https://doi.org/10.1016/j.fusengdes.2018.04.090.

[2] G. Federici, Testing needs for the development and qualification of a breeding blanket for DEMO, Nucl. Fusion 63 (2023) 125002, https://doi.org/10.1088/1741-4326/ad00cb.

[3] A. Santucci, M. Incelli, L. Noschese, C. Moreno, F. Di Fonzo, M. Utili, S. Tosti, C. Day, The issue of tritium in DEMO coolant and mitigation strategies, Fusion Eng. Des. 158 (2020) 111759, https://doi.org/10.1016/j.fusengdes.2020.111759.

[4] F.A. Hernandez, P. Arena, L.V. Boccaccini, I. Cristescu, A. Del Nevo, P. Sardain, G. A. Spagnuolo, M. Utili, A. Venturini, G. Zhou, Advancements in designing the DEMO driver blanket system at the EU DEMO pre-conceptual design phase: overview, challenges and opportunities, J. Nucl. Eng. 4 (2023) 565–601, https://doi.org/10.3390/jne4030037.

[5] N. Sakaba, T. Furusawa, T. Kawamoto, Y. Ishii, Y. Oota, Short design descriptions of other systems of the HTTR, Nucl. Eng. Des. 233 (2004) 147–154, https://doi.org/10.1016/j.nucengdes.2004.08.024.

[6] M.S. Yao, R.P. Wang, Z.Y. Liu, X.D. He, J. Li, The helium purification system of the HTR-10, Nucl. Eng. Des. 218 (2002) 163–167, https://doi.org/10.1016/S0029-5493(02)00187-5.

[7] V. Narcisi, A. Santucci, Analysis of the integral zeolite molecular sieve process for helium CPS application, Fusion Eng. Des. 202 (2024) 114321, https://doi.org/10.1016/j.fusengdes.2024.114321.

[8] S. Jovic, Y. Laxminarayan, J. Keurentjes, J. Schouten, J. van der Schaaf, Adsorptive water removal from dichloromethane and vapor-phase regeneration of a molecular sieve 3A packed bed, Ind. Eng. Chem. Res. 56 (2017) 5042–5054, https://doi.org/10.1021/acs.iecr.7b00433.

[9] Y. Wang, Measurements and modeling of water adsorption isotherms of Zeolite Linde-type a crystals, Ind. Eng. Chem. Res. 59 (2020) 8304–8314, https://doi.org/10.1021/acs.iecr.9b06891.

[10] S. Mokhatab, W.A. Poe, J.Y. Mak, Natural gas dehydration and mercaptans removal, in: S. Mokhatab, W.A. Poe, J.Y. Mak (Eds.), Handbook of Natural Gas Transmission and Processing, 4th ed., Gulf Professional Publishing, Elsevier, Waltham, MA, 2019, p. 307. Chapter 9.

[11] H.L. Bart, U. von Gemmingen, Ullmann's Encyclopedia of Industrial Chemistry, Wiley VCH, Weinheim, Germany, 2005, https://doi.org/10.1002/14356007.b03_09.pub2.

[12] A. Gorbach, M. Stegmaier, G. Eigenberger, Measurement and modeling of water vapor adsorption on zeolite 4A – equilibria and kinetics, Adsorption 33 (2004) 1375–1384, https://doi.org/10.1023/B:ADSO.0000024033.60103.ff.

[13] M. Tarantino, D. Martelli, A. Del Nevo, M. Utili, I. Di Piazza, M. Eboli, D. Diamanti, A. Tincani, G. Miccichè, D. Bernardi, F.S. Nitti, C. Cristalli, S. Bassini, A. Fiore, S. Cataldo, C. Sartorio, A. Venturini, R. Marinari, P. Lorusso, Fusion technologies development at ENEA Brasimone research centre: status and perspectives, Fusion Eng. Des. 160 (2020) 112008, https://doi.org/10.1016/j.fusengdes.2020.112008.

[14] The GPSA Engineering Data Book, 14th Edition.

[15] S. Ergun, Fluid flow through packed columns, J. Chem. Eng. 48 (1952) 89–94.

[16] Y. Wang, Measurements and modeling of water adsorption isotherms of Zeolite Linde-type a crystals, Ind. Eng. Chem. Res. 59 (2020) 8304–8314, https://doi.org/10.1021/acs.iecr.9b06891.

[17] D. Fraenkel, J. Shabtai, Encapsulation of hydrogen in molecular sieve zeolites, J. Am. Chem. Soc. 99 (21) (1977) 7074–7076, https://doi.org/10.1021/ja00463a058.

[18] N. Bouaziz, M.B. Manaa, F. Aouaini, A.B. Lamine, Investigation of hydrogen adsorption on zeolites A, X and Y using statistical physics formalism, Mater. Chem. Phys. 225 (2019) 111–121, https://doi.org/10.1016/j.matchemphys.2018.12.024.

[19] H.W. Langmi, A. Walton, M.M. Al-Mamouri, S.R. Johnson, D. Book, J.D. Speight, P. P. Edwards, I. Gameson, P.A. Anderson, I.R. Harris, Hydrogen adsorption in zeolites A, X, Y and RHO, J. Alloy. Compd. 356 (357) (2003) 710–715, https://doi.org/10.1016/S0925-8388(03)00368-2.

[20] F.V.S. Lopes, C.A. Grande, A.M. Ribeiro, J.M. Loureiro, O. Evaggelos, V. Nikolakis, A.E. Rodrigues, Adsorption of H_2, CO_2, CH_4, CO, N_2 and H_2O in activated carbon and zeolite for hydrogen production, Sep. Sci. Technol. 44 (5) (2009) 1045–1073, https://doi.org/10.1080/01496390902729130.

[21] J. Yang, L. Dehdari, Y. Guo, J. Guo, R. Singh, P. Xiao, J. Shang, A. Zavabeti, G.K. Li, Hydrogen capture using zeolite 3A for pipeline gas deblending, Chem. Eng. J. 466 (2023) 143224, https://doi.org/10.1016/j.cej.2023.143224.

[22] M. Llano-Restrepo, M.A. Mosquera, Accurate correlation, thermochemistry, and structural interpretation of equilibrium adsorption isotherms of water vapor in zeolite 3A by means of a generalized statistical thermodynamic adsorption model, Fluid Phase Equilibr. 283 (2009) 73–88, https://doi.org/10.1016/j.fluid.2009.06.003.